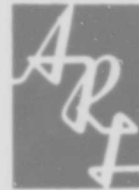


AD610509

ARL 64-207
NOVEMBER 1964



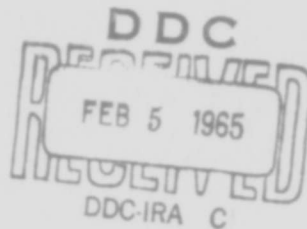
Aerospace Research Laboratories

SCHLIEREN INVESTIGATION OF THE FLOW PHENOMENA ABOUT A TWO-DIMENSIONAL CIRCULAR CYLINDER IN A HYPERSONIC FLOW

K. H. TOKEN
H. OGURO
UNIVERSITY OF CINCINNATI
CINCINNATI, OHIO

COPY	2	OF	3	<i>Vmc</i>
HARD COPY				\$. 2.00
MICROFICHE				\$. 0.50

49-P



OFFICE OF AEROSPACE RESEARCH
United States Air Force



ARCHIVE COPY

BLANK PAGE

NOTICES

When Government drawings, specifications, or other data are used for any purpose other than in connection with a definitely related Government procurement operation, the United States Government thereby incurs no responsibility nor any obligation whatsoever; and the fact that the Government may have formulated, furnished, or in any way supplied the said drawings, specifications, or other data, is not to be regarded by implication or otherwise as in any manner licensing the holder or any other person or corporation, or conveying any rights or permission to manufacture, use, or sell any patented invention that may in any way be related thereto.

- - - - -

Qualified requesters may obtain copies of this report from the Defense Documentation Center, (DDC), Cameron Station, Alexandria, Virginia.

- - - - -

This report has been released to the Office of Technical Services, U. S. Department of Commerce, Washington 25, D. C. for sale to the general public.

- - - - -

Copies of ARL Technical Documentary Reports should not be returned to Aerospace Research Laboratories unless return is required by security considerations, contractual obligations or notices on a specified document.



BLANK PAGE

ARL 64-207

**SCHLIEREN INVESTIGATION OF THE FLOW PHENOMENA
ABOUT A TWO-DIMENSIONAL CIRCULAR CYLINDER
IN A HYPERSONIC FLOW**

**K. H. TOKEN
H. OGURO**

**UNIVERSITY OF CINCINNATI
CINCINNATI, OHIO**

NOVEMBER 1964

**Contract AF 33(616)-8453
Project 7064**

**AEROSPACE RESEARCH LABORATORIES
OFFICE OF AEROSPACE RESEARCH
UNITED STATES AIR FORCE
WRIGHT-PATTERSON AIR FORCE BASE, OHIO**

FOREWORD

This interim technical report was prepared by the University of Cincinnati, Hypersonic Aerodynamics Research Staff on Contract AF 33(616) 8453, titled, "Experimental Aerothermodynamic Investigations," for the Aerospace Research Laboratories, Office of Aerospace Research, United States **Air Force** . The work reported herein was accomplished under Project 7064, "Aerothermodynamic Investigations in High-Speed Flow," during the period between December 1962 and August 1963, and is the first of a two report series dealing with the subject. Colonel Andrew Boreske, Jr., Deputy Commander of the Aerospace Research Laboratories, served as Project Monitor for this work.

ABSTRACT

This paper describes an experimental investigation of the fluid flow phenomena about a two-dimensional circular cylinder in a hypersonic stream. The data presented was accumulated solely through the use of the Schlieren technique of flow visualization. The primary purpose of the investigation was to document the variation of the flow pattern with respect to flow parameters and models employed. As a result, the determination of specific problems for future investigation can be more adequately defined. Data concerning stagnation point shock layer thickness, bow shock wave shape, secondary shock wave shape, initial viscous wake growth, shear layer surrounding the base flow region, and intrinsic properties of the models and facility used are presented and discussed. All tests were conducted at a nominal free stream Mach Number of 14, while the free stream Reynolds Number was varied from 0.32×10^4 to 6.44×10^4 . Reynolds Number variation was achieved by holding total temperature constant, ranging total pressure from 800 to 2000 psia, and changing model diameters from 1/8 to 3/4 inch.

TABLE OF CONTENTS

Section		Page
I	INTRODUCTION	1
II	DESCRIPTION OF THE EXPERIMENTAL METHOD	2
	EXPERIMENTAL MODELS	5
	SCHLIEREN TECHNIQUE	9
	TEST PROCEDURE	10
	PHOTOGRAPHIC EQUIPMENT	11
	DATA REDUCTION	12
III	DISCUSSION OF RESULTS	14
	BOW SHOCK WAVE	23
	SHOCK LAYER THICKNESS	23
	WAKE NECK REGION	23
	WAKE SHOCK WAVE	29
	INITIAL WAKE GROWTH	32
	THE INITIAL FLOW PATTERN	32
	THE SECOND FLOW PATTERN	35
IV	CONCLUSIONS	36
	BOW SHOCK WAVE STANDOFF DISTANCE	36
	INITIAL AND SECOND FLOW REGIMES	36
	SUGGESTIONS FOR FUTURE INVESTIGATION	36
V	BIBLIOGRAPHY	38
VI	REFERENCES	39

LIST OF ILLUSTRATIONS

Figure	Page
1. Schematic Diagram of Wind Tunnel and Schlieren System	3
2. Photograph of Models	6
3. Photograph of Test Cabin with Model Installed	8
4. Schlieren Photograph of Initial Flow Pattern	16
5. Schlieren Photograph of Second Flow Pattern	17
6. Schlieren Photograph of Initial Flow Field	18
7. Schlieren Photograph of Second Flow Field	19
8. Schlieren Photograph of Initial Flow Pattern	20
9. Schematic Diagram of Flow Configuration	22
10. Bow Shock Wave Shape	24
11. Bow Shock Wave Stand-Off Distance vs. Reynolds Number	25
12. Distance to Wake Neck vs. Reynolds Number; Initial and Second Flow Regimes	26
13. Wake Neck Width vs. Reynolds Number; Initial and Second Flow Regime	27
14. Effect of Reynolds Number and Model Diameter on Shear Layer Geometry	28
15. Shear Layer Angle vs. Reynolds Number; Initial and Second Flow Pattern	30
16. Wake Shock Shape; Second Flow Pattern	31
17. Wake Shock Shape; Initial Flow Pattern	33
18. Wake Growth; Initial Flow Pattern	34

NOMENCLATURE

Y	Coordinate normal to free stream flow measured from body axis.
X	Coordinate parallel to free stream flow measured from body axis.
R_e	Reynolds Number.
Δ	Bow shock wave stand off distance.
d	Body diameter
v	Stream velocity.
θ	Mean shear angle with respect to flow direction.
T	Temperature.
P	Pressure.
M	Mach Number.

Subscripts:

- S - Forward stagnation point values.
- O - Wake neck values.
- b - Body surface conditions.
- t - Total conditions.

I INTRODUCTION

The properties of the viscous wake associated with bodies traveling at hypersonic speeds are determined by the flow history of the fluid particles contained within it. A fluid particle contained within the boundary layer of such bodies experiences a comparatively long shear flow history relative to body size before entering the so called far wake. These shear flows which the fluid particle experiences can, for purposes of discussion and analysis, be categorized into the boundary layers, the shear layers between boundary layer separation and reattachment, the base flow region inside the shear layers, the reattachment or wake neck region, and the near wake where the inviscid wake acts to accelerate the viscous wake. Lateral inconsistency among data obtained from experiments in the far wake may well be due to entirely different shear flows which fluid particles experience before entering that region.

The formulation of assumptions concerning the thermodynamic and fluid dynamic parameters at the wake neck is characteristic of most current theoretical analysis of the hypersonic wake. Due to the relatively small amount of data available in this region, the aforementioned assumptions have not been experimentally confirmed.

The purpose of this paper is to quantitatively evaluate the effects of varying the flow parameters at the body and in the free stream on the shear flows which form the viscous wake. Initial experiments employed the schlieren flow visualization technique. The data presented herein was obtained solely by this method.

The body configuration tested was a two-dimensional circular cylinder in a full span across the test gas stream. This choice was based on simple body geometry, which lends itself to ease in

"Manuscript released September 1964 by the authors for publication as an ARL technical documentary report.

manufacture. Further, the full span configuration negates end effects on the center portion of the models and affords inherently simple access for instrumentation leads which were planned for later tests.

The entire experimental program was conducted in the twenty-inch diameter hypersonic wind tunnel located at the Aerospace Research Laboratories and was limited to testing at Mach number 14, the present Mach number capability of this facility.

Although the primary purpose of the investigation, as stated above, was to determine variations in shear layer flows, the Schlieren technique resulted in density gradient information for the entire flow field. Thus, very little additional data reduction resulted in information on the shock patterns involved.

The results obtained, therefore, afford information on bow shock wave shape and standoff distance. The fluid mechanic variations of the wake neck region are also documented.

As a result of this work, areas of further investigation are defined.

II DESCRIPTION OF THE EXPERIMENTAL METHOD

The twenty-inch diameter hypersonic tunnel located at the Aerospace Research Laboratories is of the axisymmetric, open jet, and blow-down type (See Figure 1). The 3000 psi high pressure air supply was, for this series of tests, reduced to tunnel stagnation pressures ranging from 800 to 2000 psia. Air, at the selected stagnation pressure, was heated in the resistance type heater until the heat transfer mechanism had reached an equilibrium condition. The stagnation temperature for all experiments was the maximum obtainable, namely, 1800° R (nominal at nozzle reservoir). During heater stabilization, the heated air was exhausted through a bypass valve designed to accommodate a mass flow identical to that of the tunnel flow nozzle. Simultaneously, the nozzle, test chamber, diffuser, and all

Stations

- 1 Reservoir Supply Pressure
- 2 Heater
- 3 Hot Valve
- 4 Bypass Valve
- 5 Nozzle Throat
- 6 Test Cabin
- 7 Line To Vacuum Pumps and Vacuum Sphere

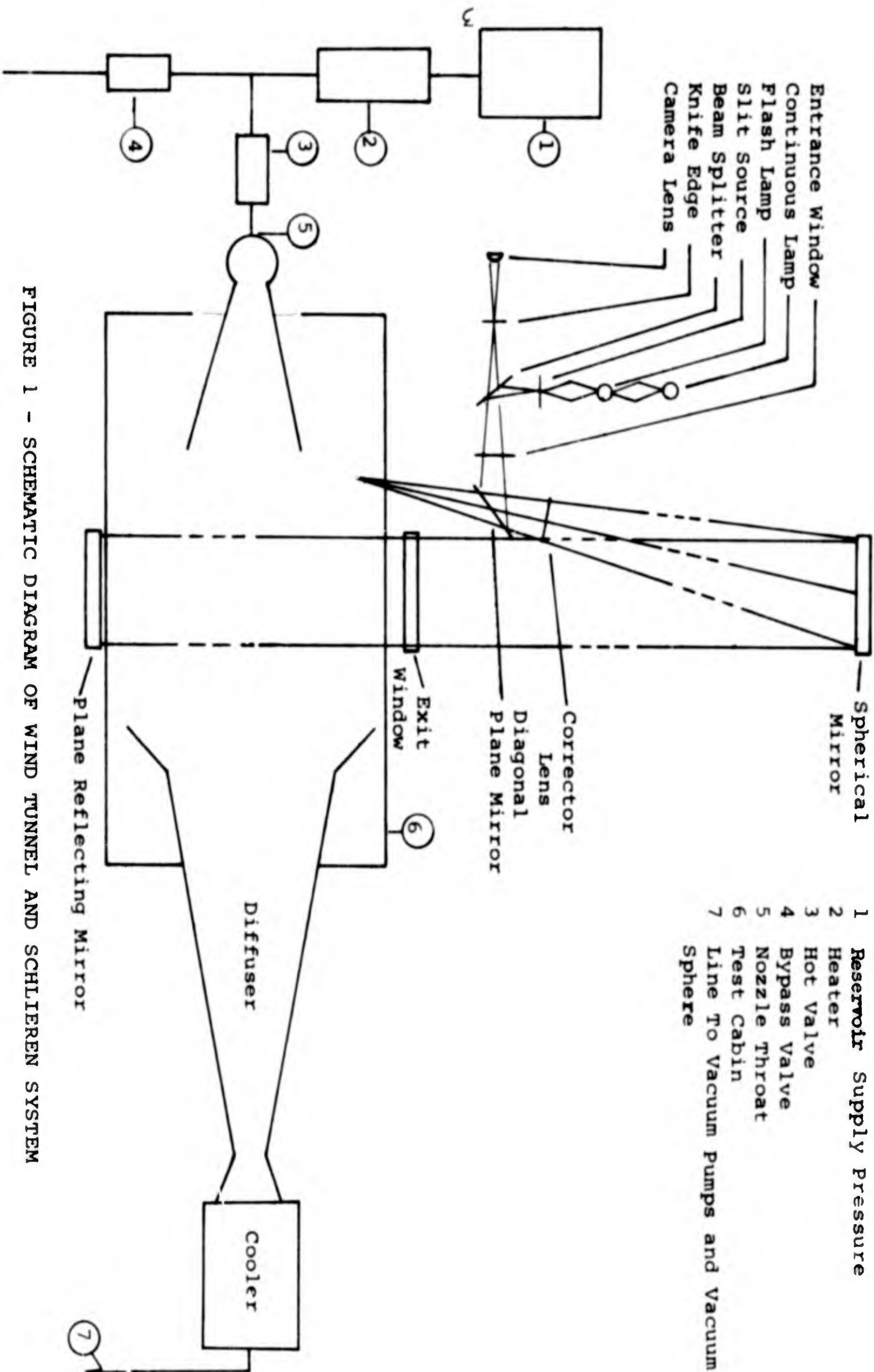


FIGURE 1 - SCHEMATIC DIAGRAM OF WIND TUNNEL AND SCHLIEREN SYSTEM

associated piping to the vacuum system was exhausted to approximately 2 millimeters of mercury. The vacuum system for this facility consists of a series of rotary vane type pumps and a 35,000 cubic foot storage sphere. The minimum pressure obtainable was approximately 1/2 millimeter of mercury.

The hot-valve, the device used to seal the stagnation pressure region from the exhausted components of the tunnel, was then opened and the tunnel flow reached equilibrium after the starting shock system was forced into the divergent section of the diffuser. Running duration times for these experiments reached a maximum of approximately 200 seconds. Usually, however, tunnel running times averaged 60 to 80 seconds. These run durations were determined by the ability of the vacuum system to maintain a low exhaust pressure. Tunnel runs were terminated using the empirical parameter which states: When test chamber static pressure reaches a value of four times the free stream pressure, the tunnel can no longer support Mach 14 flow. This parameter was based on the fact that at pressure ratios above this value, shock waves issuing from the nozzle reach too far into the test section. Certainly then, run time duration was increased with decreased total pressure and model size. The total number of runs obtainable during any one day was determined by the ability of the pumps in the vacuum system to remain cool enough so as not to seize.

All models were located at a nominal distance of 4 inches from the nozzle exit plane. At this location a 3.2 percent variation in Mach Number was observed for a total pressure range of 600 to 2000 psia. Operational difficulties connected with the air heater in this tunnel held the maximum total temperature to 1800° R and resulted in a total temperature variation of $\pm 50^{\circ}$ R about the 1800° R nominal value. A maximum variation in Mach Number of 0.36 percent was observed at a total pressure of 800 psia. Since all data taken was of a qualitative type, these variations in Mach Number were resolved as negligible.

Data accumulated by the University of Cincinnati Hypersonic Research Staff indicates that liquefaction presents no problem at the total pressures and temperatures employed.

A more complete description of the facility, along with its associated equipment and flow nozzle calibrations, can be found in References 1 through 4.

EXPERIMENTAL MODELS

A two-dimensional circular cylinder body configuration at full span imposes definite alignment problems for the Schlieren technique. This body configuration, however, was chosen as being more suitable to the experimental work which will be defined as a result of the Schlieren analysis. Geometrically, all models are inherently simple, however, three distinct types were employed, (See Figure 2).

Primary models, or models from which the bulk of the data was obtained, were constructed from solid rods of type 304 stainless steel. All of these models had constant diameter sections 22.5 inches long, and at each end a 1/2 inch long by 1/4 inch diameter section for mounting. The 22.5 inches long constant diameter sections were 1/8, 3/16, 1/4, 5/16, 3/8, 1/2 and 3/4 inches in diameter with a tolerance of ± 0.0005 inch. The surface finish of these models was "as delivered" except that stock with scratches was rejected.

Boundary layer trip models were employed in an effort to turbulate the boundary layer. These models were further divided into three types wherein a 3/8 inch primary type model was used as the base model in each case. The first type was constructed by the resistance welding of 0.003 inch diameter iron wires at plus and minus 15 degrees on either side of the forward stagnation point of a base model. This model failed due to inadequate welding technique, since the trip wires broke loose when the starting shock system proceeded through the test chamber.

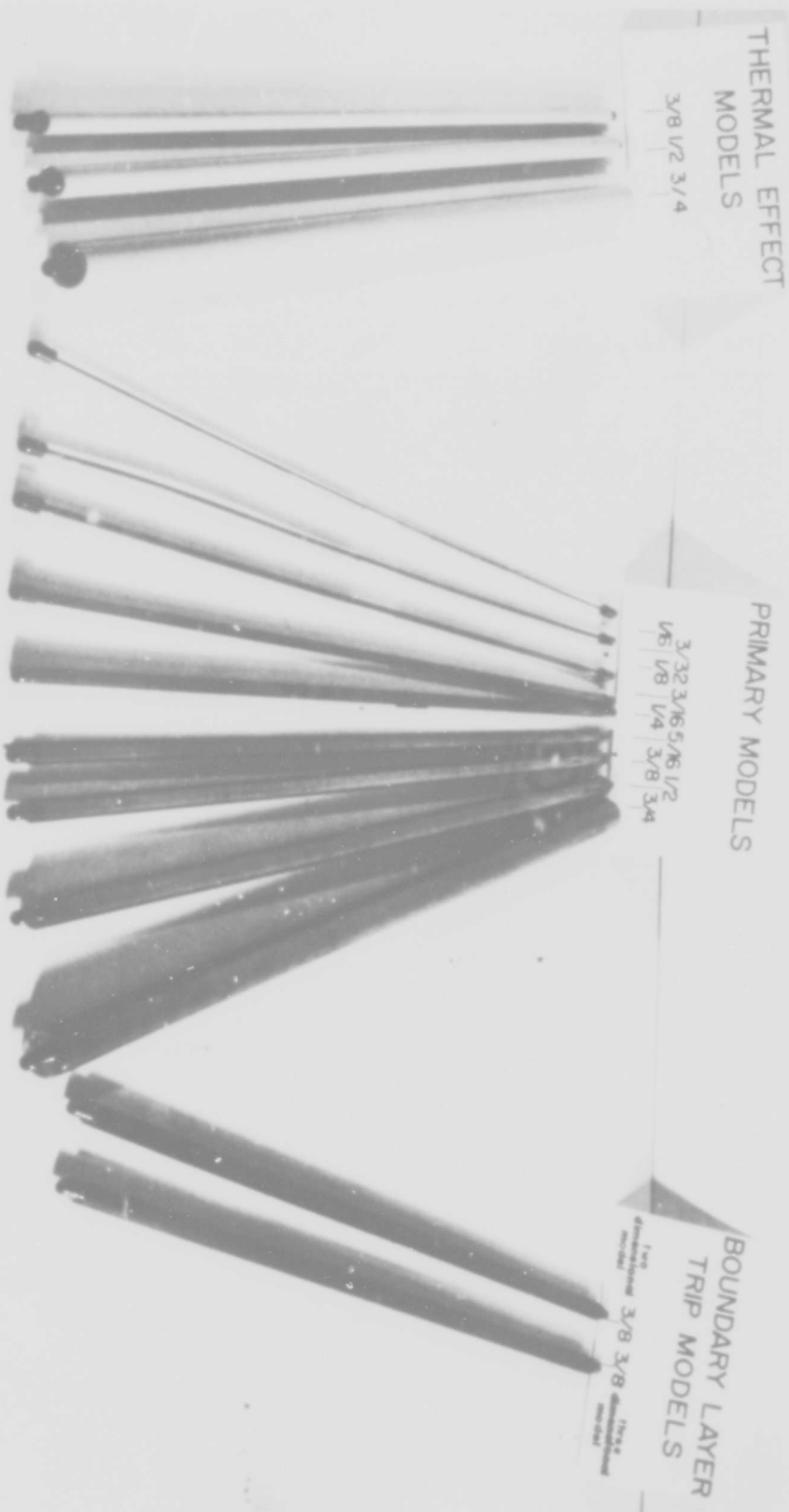


FIGURE 2 - PHOTOGRAPH OF MODELS

The second type of boundary layer trip model was of the three-dimensional roughness type. This roughness was obtained by sand blasting the entire surface of the constant diameter section of a base model. The roughness produced was estimated as 0.002 inch peak to peak.

As a third model, a more sturdy two-dimensional roughness type model was constructed. This model was manufactured by machining 60 degree included angle grooves, 0.007 inch deep, every 2 1/2 degrees through an arc of plus and minus 90 degrees about the stagnation point of a base model.

A third type model was designed based on a suspected thermal effect. This type of model utilizes a vitreous refractory mullite outer tube, 1/8 inch thick, which is supported by an appropriate outer diameter drill rod. The outer shell has a thermal conductivity of 1.45 Btu ft/hr ft²°F. Comparing this to the type 304 stainless steel primary models with a thermal conductivity of 12.4 Btu ft/hr ft²°F, it can be seen that an equilibrium surface temperature would be reached more rapidly than with the stainless steel models. These models were constructed in 3/8, 1/2, and 3/4 inch outer diameters.

All models were supported with the system herein described. An illustration of the model support installed in the tunnel test chamber is shown in Figure 3. As shown, a 1/8 inch thick, 3 1/2 inches wide, steel circumferential strap was clamped about the nozzle near the exit by means of tightening bolts. Two adjustable "T" plates were then bolted to diametrically opposed parallel surfaces. The "T" plates accommodate adjustment in the plane of the parallel surfaces by moving along the slots provided. The models lay perpendicularly between the "T" plates with their 1/4 inch diameter end pieces resting in holes provided. Set screws restricted model movement in these holes. In order to hold these models vertically, the circumferential strap was simply rotated through 90 degrees. Thus, all models in either a horizontal or a vertical position extended one inch beyond the free jet boundary.

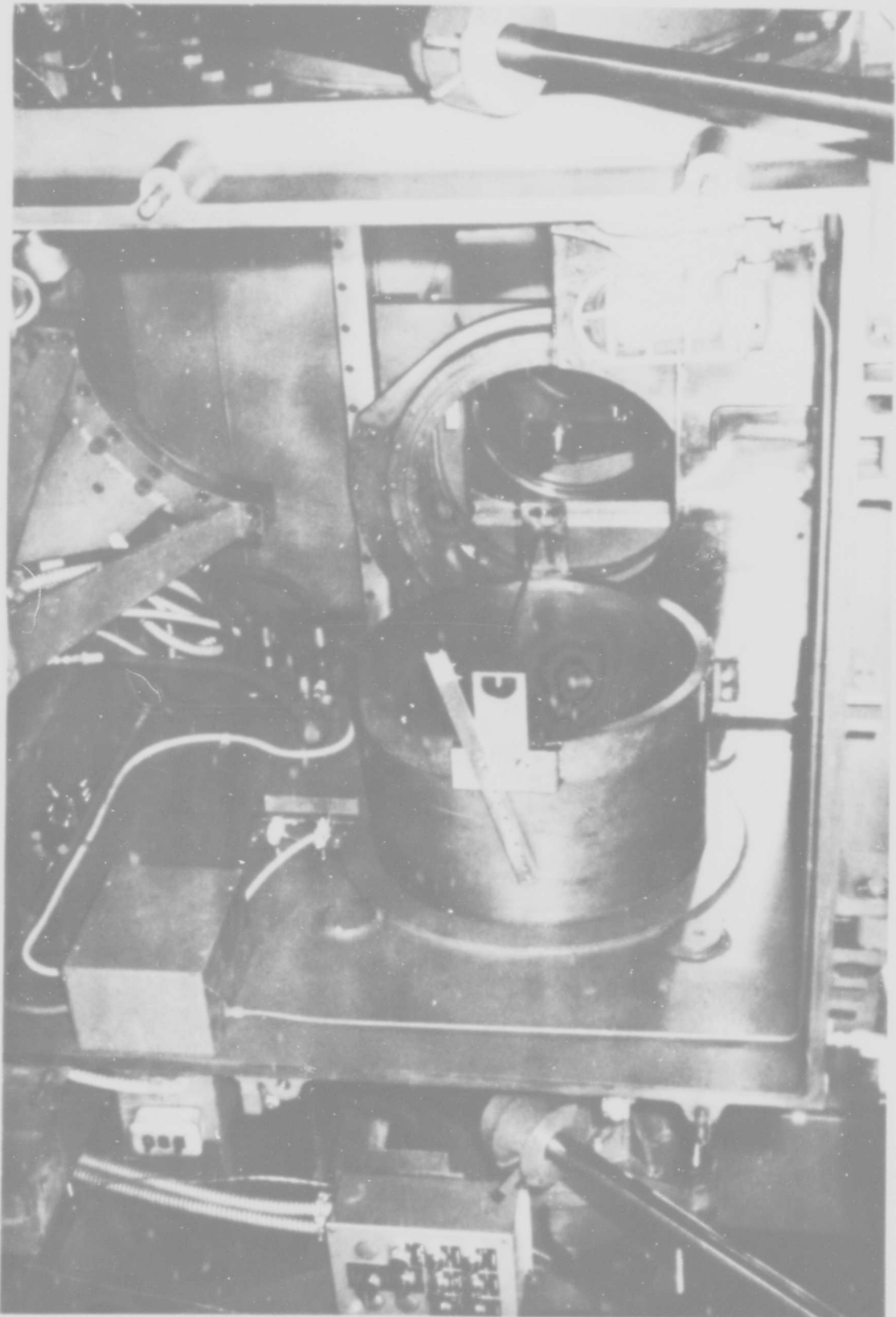


FIGURE 3 - PHOTOGRAPH OF TEST CABIN WITH MODEL INSTALLED (FLOW DIRECTION RIGHT TO LEFT)

In addition, provisions were made to attach scaling devices of known size into the Schlieren System's field of view, thus serving to scale all Schlieren results to actual dimensions. Additionally, these scaling devices minimized error in photographic or optical manipulation of data during its reduction.

SCHLIEREN TECHNIQUE

The Schlieren System used as the sole experimental tool for these tests was designed and built by Wacline Inc. of Optron Laboratory in Dayton, Ohio. A brief description of the System components and their control can be found in Reference 5. As is common in dealing with flows of lower density, the Schlieren System designed for the twenty-inch hypersonic tunnel is of the double pass type. The System also utilizes the off axis principle. Instead of an off axis parabolic mirror, economic considerations afford the System with a spherical mirror in conjunction with an aspheric lens to compensate for aberrations. All optics, with the exception of the plane reflecting mirror, are situated on a carriage which is located on one side of the tunnel test chamber, while the reflecting mirror is on the opposite side and can be remotely adjusted. Admission of the Schlieren beam through the test chamber is obtained through use of 14 inch diameter crown glass windows with optical deviations from a spherical wave front not exceeding $1/4$ second angle. Two light sources are available for use: An Osram HBO 200W L-2 Super Pressure Mercury Lamp affords a continuous light source while a Xenon flash lamp, G.E. FT203, affords light durations of approximately 10 microseconds. These light sources are positioned and focused with lenses such that either can be used once the light source knife edge is adjusted. The geometric arrangement of the components mentioned above along with accompanying equipment is depicted in Figure 1.

TEST PROCEDURE

This section deals with the procedures used for model and Schlieren System alignment. A discussion of inherent errors induced by uncontrollable factors in data accumulation is presented.

Through the use of a 100 centimeter cathetometer, models could be positioned within 0.004 inch of the tunnel centerline and made level to within 2 minutes of arc in the vertical plane. In the horizontal plane a vernier scale was used to position models to within 20 minutes of arc with respect to the nozzle exit plane.

Measurements indicate that the nozzle exit plane is within 25 minutes of arc of being vertical. Considering the manufacturing technique employed in its construction, a good approximation would indicate that the horizontal plane is also within the same 25 minutes of arc of being perpendicular to the mean flow direction. A further assumption that the nozzle exit plane is perpendicular to the test chamber walls allows proper alignment of the Schlieren collimating tube with the experimental model. This latter assumption was partially born out in that visual inspection of the Schlieren image indicated good alignment.

The Schlieren System collimating tube was aligned to the true horizontal through the use of a level graduated in increments of 0.0005 inch per foot and the screw type jacks designed for this purpose at the four corners of the collimating tube carriage. The tube was also aligned perpendicularly to the test chamber walls, by the use of a vernier scale, to within 25 minutes of arc. In later experiments visual monitoring of the Schlieren image was used exclusively during Schlieren System alignment.

The reasons for the somewhat cautious procedure outlined above, for alignment of the model and Schlieren tube, become apparent upon consideration of the two-dimensional type model

spaning 20 inches of flow. Slight misalignments could easily have preempted any worthwhile measurements from being taken from the Schlieren photographs obtained. The more obvious error is the possibility of superimposed density gradients on the photographic film. Just as serious is the possibility of the obliteration of detail due to reflection of the light from model surfaces not parallel to the Schlieren light path. A detailed discussion of possible errors involved with the Schlieren technique may be found in References 5 and 7.

Once Schlieren System alignment had been accomplished, adjustment of Schlieren optical components remained in order to obtain results of an adequate caliber. Adjustment of the plane reflecting mirror was accomplished easily, since the only requirement was that it return reflected Schlieren light parallel to incident light. To accommodate this plane mirror adjustment, cross hairs are permanently installed in the collimating tube in front of the spherical mirror. When the cross hairs appeared coincident in the eye piece, incident and reflected light beams on the plane mirror were parallel. The knife edge carriage was then located axially at the focal point of the secondary image. This adjustment was considered complete when the point had been reached where, with adjustment of the knife edge transverse to the light path, the viewing field increased or decreased in illumination in a uniform manner. The camera, with film installed, was then focused according to the test being conducted. For tests employing a vertical model, the camera was focused to the plane of the model. With horizontally oriented models, the camera was focused to the plane of the calibrating device which was located on the same side of the flow as the camera.

PHOTOGRAPHIC EQUIPMENT

The camera employed for monitoring the Schlieren System was a 35 mm. Leica especially adapted with an automatically retracting

frosted glass viewing piece and flash lamp trigger. In conjunction with that camera, two types of film were considered. Kodak Plus-X Pan Film was considered for its characteristic of high contrast and Kodak Tri-X was considered for its high speed (2200 with development used). With both the continuous light source, at any camera shutter speed, and with the flash light, Tri-X was found to have sufficient contrast and was therefore selected due to its having a higher speed than Plus-X. For the camera-film combination indicated, Schlieren light source strength was found by a trial and error process.

All films were developed using the inhouse capabilities at the Aerospace Research Laboratories. In order to obtain a speed of 2200 from the Kodak Tri-X Film, the following solutions and procedures were employed:

Developer - Kodak D19 at 20°C for 6 minutes, water rinse.

Kodak rapid fixer at 20°C for 6 minutes.

Water wash at 20°C for 30 minutes.

Forced air dry for 2 hours.

The procedure outlined above can be found in Reference 8.

DATA REDUCTION

Several types of procedure and apparatus were employed for data reduction. Error analysis concerning physical measurements of the type conducted has little significance; rather, the least count of the instruments used will be indicated.

Basically two types of photographic results were analyzed: The negative and the positive which resulted from a printing of the negative. In all cases, the bulk of the measurements were taken from the positive for sake of expediency. With the positive, inherent error exists by way of a magnification of the grain size of the negative through enlargement, and the added effect of the grain size of the positive itself. Additionally, if the negative is not completely in a plane normal to the

printing light during enlargement, distortion results. It should be noted that this latter effect is somewhat compensated by the use of calibrating devices at the time the picture is taken. In its favor, taking data from positives allows the use of more commonplace least count instruments. On the other hand, measurements taken from photographic negatives, while minimizing grain size and distortion problems, require fine instruments and considerably much more time.

The majority of the data points established to define shock wave stand off distance were determined with the use of a Gaertner Scientific Company optical comparator. This instrument features a least count of 0.0001 inch on both axes, while angular position may be easily estimated to within 10 minutes of arc. Photographic prints roughly 3 inches square were measured. The primary difficulty encountered was that of determining the exact position of the edge of the shock wave, since grain size effects were already quite noticeable and parallaxing introduced human error.

For data other than the aforementioned shock wave stand off distance, 8 1/2 by 11 inch photographic prints were measured using a 2-power magnifying glass and a scale with a least count of 1/60 of an inch. These measured dimensions were an order of magnitude larger than shock wave stand off distance and did not require a fine least count instrument.

As a check on measurements taken by the two procedures defined above, an Ansco Model 4 automatic recording microdensitometer was used in conjunction with photographic negatives mounted in slide jackets to keep them in a plane normal to the light path in the densitometer. The light source in this instrument can be adjusted in intensity, size, and shape and directed into an illuminating microscope. The illuminating microscope directs this beam of intense light onto the film negative which is mounted in a movable carriage. The carriage can be moved in its plane manually for position or automatically during actual recording.

A second microscope on the opposite side of the slide directs the light to a penta prism which projects the image on an aperture plane located directly in front of a photomultiplier. The output of the photomultiplier is connected to a constant speed strip chart recorder. In operation, plots corresponding to the first derivative of the density against spatial coordinates are accurately obtained. The aperture size in the rear image plane can be reduced to an effective aperture size of a few tenths of a micron. Between the rear image plane and the rear microscope, a reflex mirror may be introduced for visual inspection. The effective least count of this instrument, as used, was approximately one micron.

III DISCUSSION OF RESULTS

All results presented were obtained at a nominal free stream Mach Number of 14 and total temperature of 1800°R . As the total pressure and model diameters were varied, the free stream Reynolds Number correspondingly ranged from 0.322×10^4 to 6.44×10^4 . These bounds on the free stream Reynolds Number correspond to a variation of the forward stagnation point Reynolds Number between 2.05×10^2 and 30.7×10^2 , respectively.

Schlieren observation of the flow about the primary models indicated that two successive, distinctly different, flow patterns occurred chronologically during each tunnel run. Variations in stagnation pressure and temperature and in model diameter resulting in a full Reynolds Number range excursion did not noticeably alter the duration of these flow regimes. The initial flow pattern about the primary models was on the order of 6 to 7 seconds in duration. Directly thereafter the pattern changed in basic character to the second type which persisted for the remainder of the tunnel run.

Since variations in free stream conditions and model diameter had negligible effect on these flow pattern durations, several

techniques which altered surface conditions were employed. Two types of surface roughness models, two-dimensional roughness and three-dimensional roughness, were employed over the Reynolds Number range. Although a slight decrease in initial flow regime duration was observed, while employing these surface roughness models, no great effect was found.

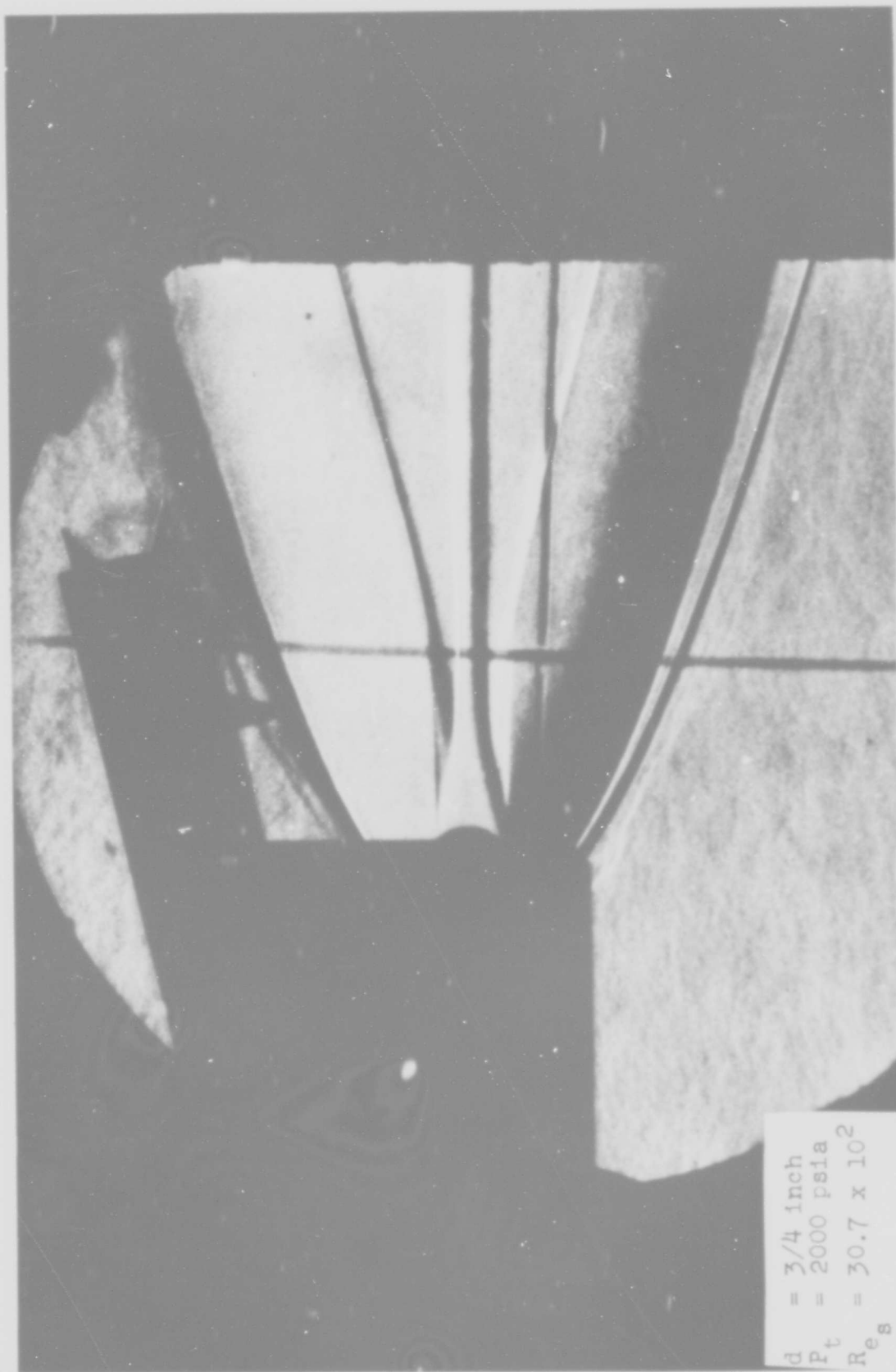
Surface temperature, a second surface parameter, was altered by the use of a ceramic surface model which produced equilibrium surface temperatures faster than the primary models. Since the ceramic has a lower coefficient of thermal conductivity than the stainless steel, energy loss from the flow by conduction from the model's surface to the interior was considerably reduced. Through the use of the ceramic model, the initial flow regime duration was decreased to 30 to 40 percent of that obtained using primary models. This result indicates the strong thermodynamic-fluid mechanical interrelationships.

Figure 4 is a Schlieren photograph of the initial flow pattern, and Figure 5 a Schlieren photograph of the second flow pattern which constitutes the majority of the tunnel run duration.

It should be noted that there exists a fundamental difference in the shear layer near wake structure. Both photographs indicate a closed wake. Further observation indicates basic differences in the density gradients behind the bow shock wave.

The Schlieren photographs of Figures 6 and 7 were obtained utilizing mounting plates which allowed observation of the bow shock wave in the forward stagnation point region. Careful analysis of Figure 6 obtained during the initial flow regime indicates the existence of a shock wave system issuing from the body in the region between the stagnation point and 90 degrees away from stagnation. No such shock system is discernable in Figure 7 which was taken during the second flow regime. Such a shock system is compatible with the results of Figure 4.

Figure 8 again depicts the initial flow pattern; however, due to the relatively small size of the model, it allows an



$d = 3/4$ inch
 $P_t = 2000$ psia
 $Re_s = 30.7 \times 10^2$

FIGURE 4 - SCHLIEREN PHOTOGRAPH OF INITIAL FLOW PATTERN

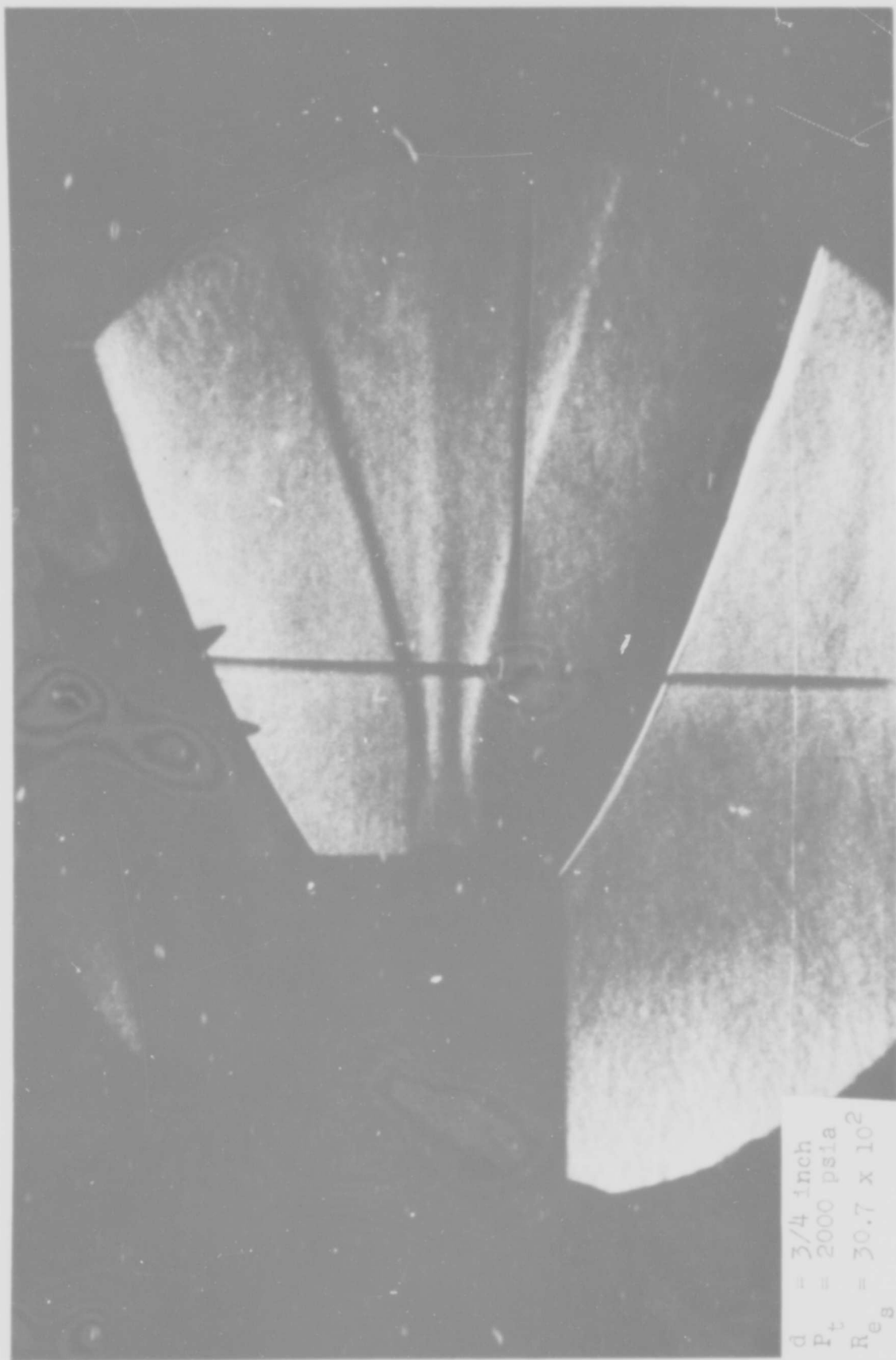
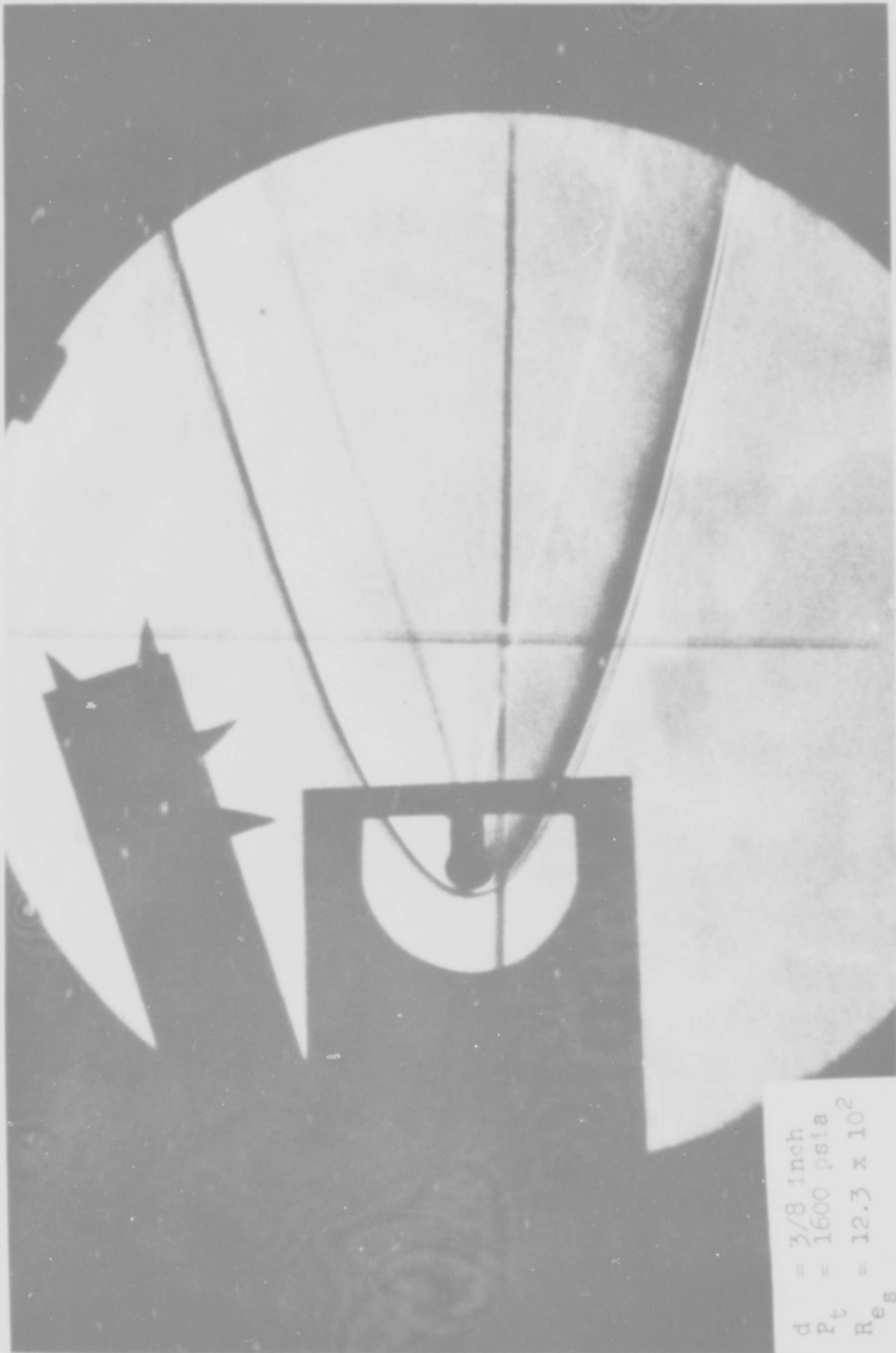
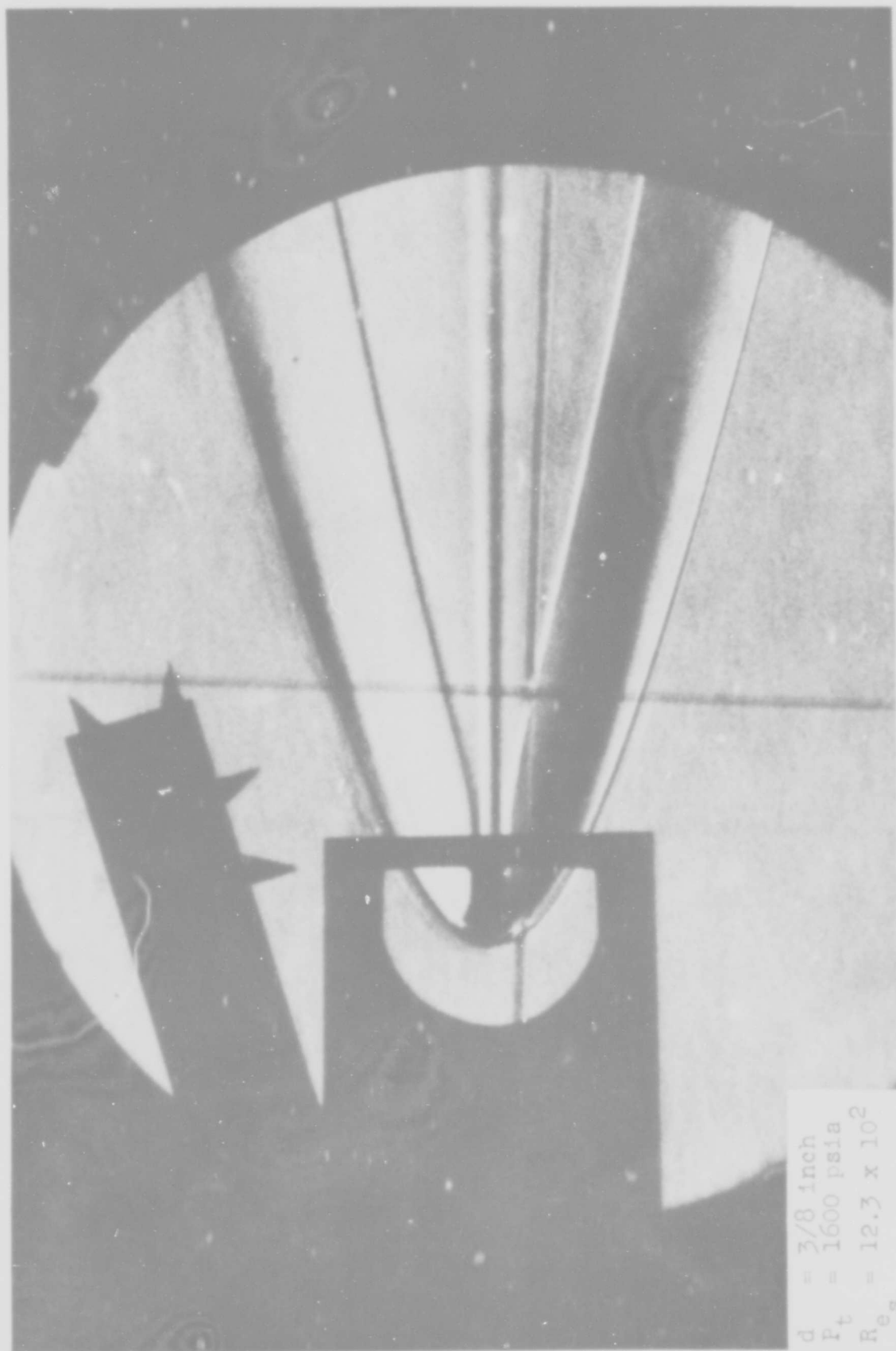


FIGURE 5 - SCHLIEREN PHOTOGRAPH OF SECOND FLOW PATTERN



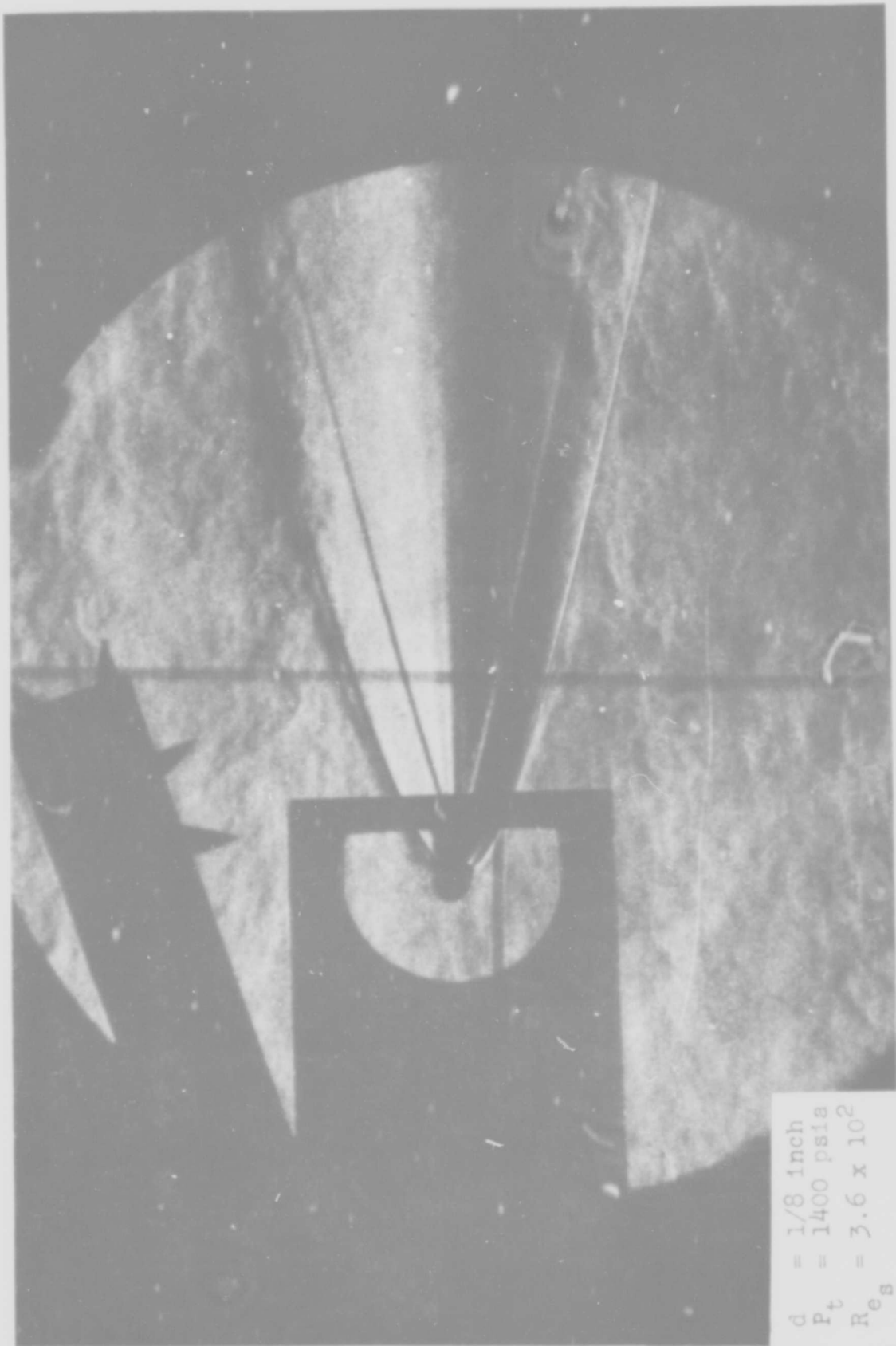
$d = 3/8$ inch
 $P_t = 1600$ psia
 $Re_s = 12.3 \times 10^2$

FIGURE 7 - SCHLIEREN PHOTOGRAPH OF SECOND FLOW FIELD



$d = 3/8$ inch
 $P_t = 1600$ psia
 $Re_s = 12.3 \times 10^2$

FIGURE 6 - SCHLIEREN PHOTOGRAPH OF INITIAL FLOW FIELD



$d = 1/8$ inch
 $P_t = 1400$ psia
 $R_{es} = 3.6 \times 10^2$

FIGURE 8 - SCHLIEREN PHOTOGRAPH OF INITIAL FLOW PATTERN

analysis of the wake at large x/d values downstream. Further, the fineness of this model in all probability introduces large model deflections and some instabilities. In addition, some model misalignment is evident. Nevertheless, the shock system issuing from the body surface is still evident. In addition, if one were to objectively pick the "point" of what appears to be laminar to turbulent transition in the wake, after the manner of Slattery and Clay, (Ref. 9), it would occur at $x/d = 30$. This result would agree with the results of Demetriades (Ref.10) who employed a hot wire to determine the transition region.

It should be noted that the Schlieren results of Figures 3 through 7 were not deemed adequate for purposes of data acquisition due mainly to Schlieren misalignment. However, because of their relatively good contrast they were chosen for the report in order to afford the reader a phenomenological understanding of the basic differences between the two flow patterns.

The 10 microsecond flash duration lamp was employed for all Schlieren pictures and thus one finds spurious density gradients on all results, especially in the bow shock wave. The facility employs fiber fax insulation in the heater and particles of this material on the order of 0.01 inch in diameter have been found imbedded on model surfaces. It is possible that these particles in the vicinity of the model cause the extraneous density gradients.

Microdensitometer traces across the entire flow pattern were obtained. Integration of these traces was attempted in an effort to obtain density profiles across the two flow regimes. However, grain size and non-linearity effects on the film did not afford a consistent result. The technique was therefore abandoned. Having thus established the differences between the two regimes, let us turn to results obtained within each regime. Figure 9 depicts the general flow configuration surrounding the two dimensional cylinder. The variables thereon defined hold true throughout the report.

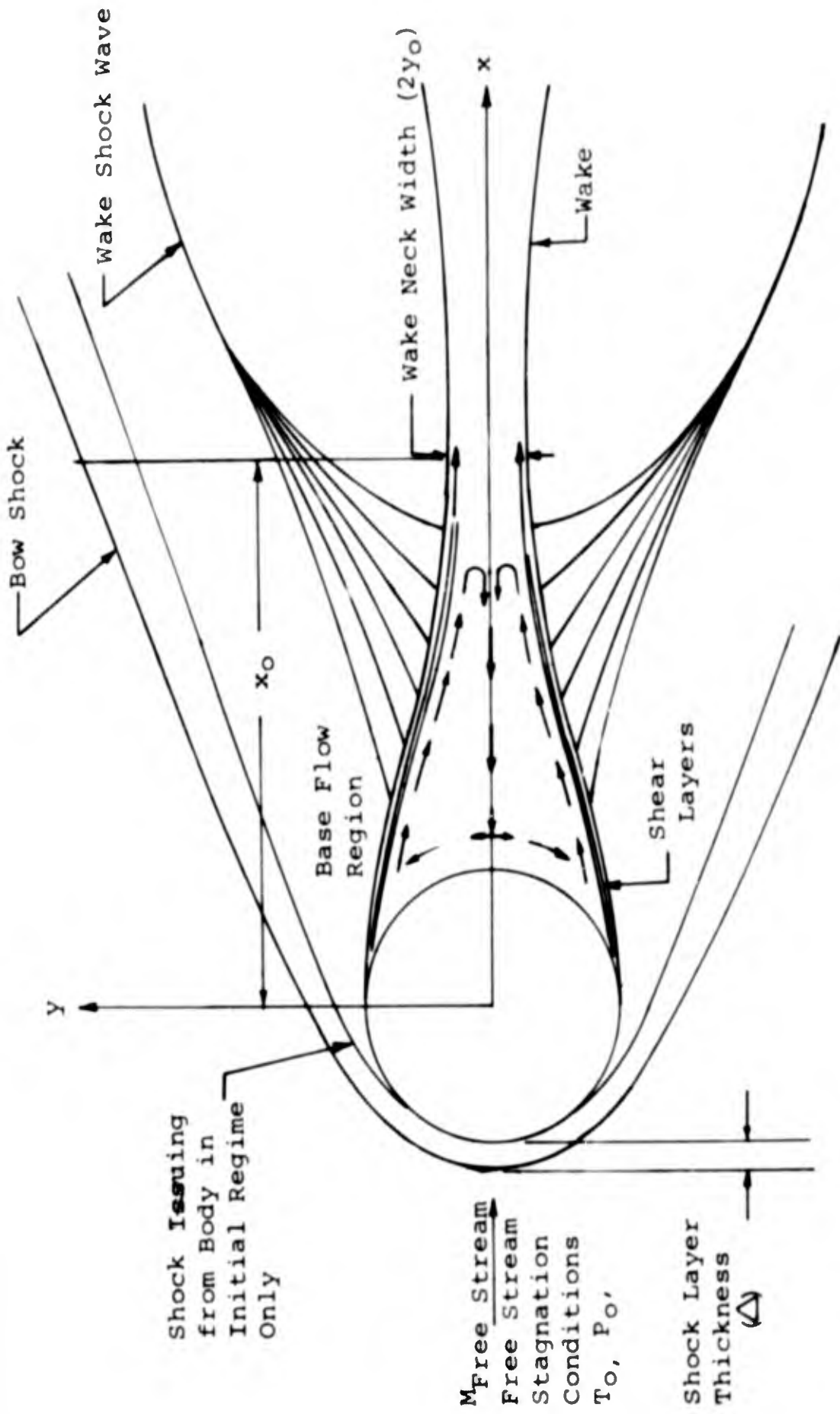


FIGURE 9 - SCHEMATIC DIAGRAM OF FLOW CONFIGURATION

BOW SHOCK WAVE

Figure 10 depicts the bow shock wave shape non-dimensionalized with respect to body diameter. As shown, the data is invariant with flow regime, type of body surface or Reynolds Number. Also shown on the figure are two parabolas such that the approximate shape of the bow shock wave might be appreciated. Since the bow shock wave is invariant with Reynolds Number, thin shock wave assumptions may be applicable.

SHOCK LAYER THICKNESS

At the stagnation point the shock layer thickness was found to be independent of Reynolds Number within the tolerances of measurement. This result is shown on Figure 11. The shock layer thickness was obtained with the model oriented vertically. Thus, the Schlieren light was perpendicular to it. This result was again obtained utilizing a photomultiplier device in conjunction with the Schlieren system, (Ref. 14). The excellent agreement between the two techniques adds considerably to confidence in both.

WAKE NECK REGION

Figures 12 and 13 combine to describe the wake neck region. Figure 12 depicts the distance to the wake neck from the body as increasing with Reynolds Number in the initial flow regime. The wake neck width during the initial flow regime is shown to decrease with Reynolds Number on Figure 13. Thus, for a given constant total pressure, the effect of model size is shown in Figure 14 (a). Whereas with constant diameter and variations in total pressure, the flow geometry is shown in Figure 14 (b).

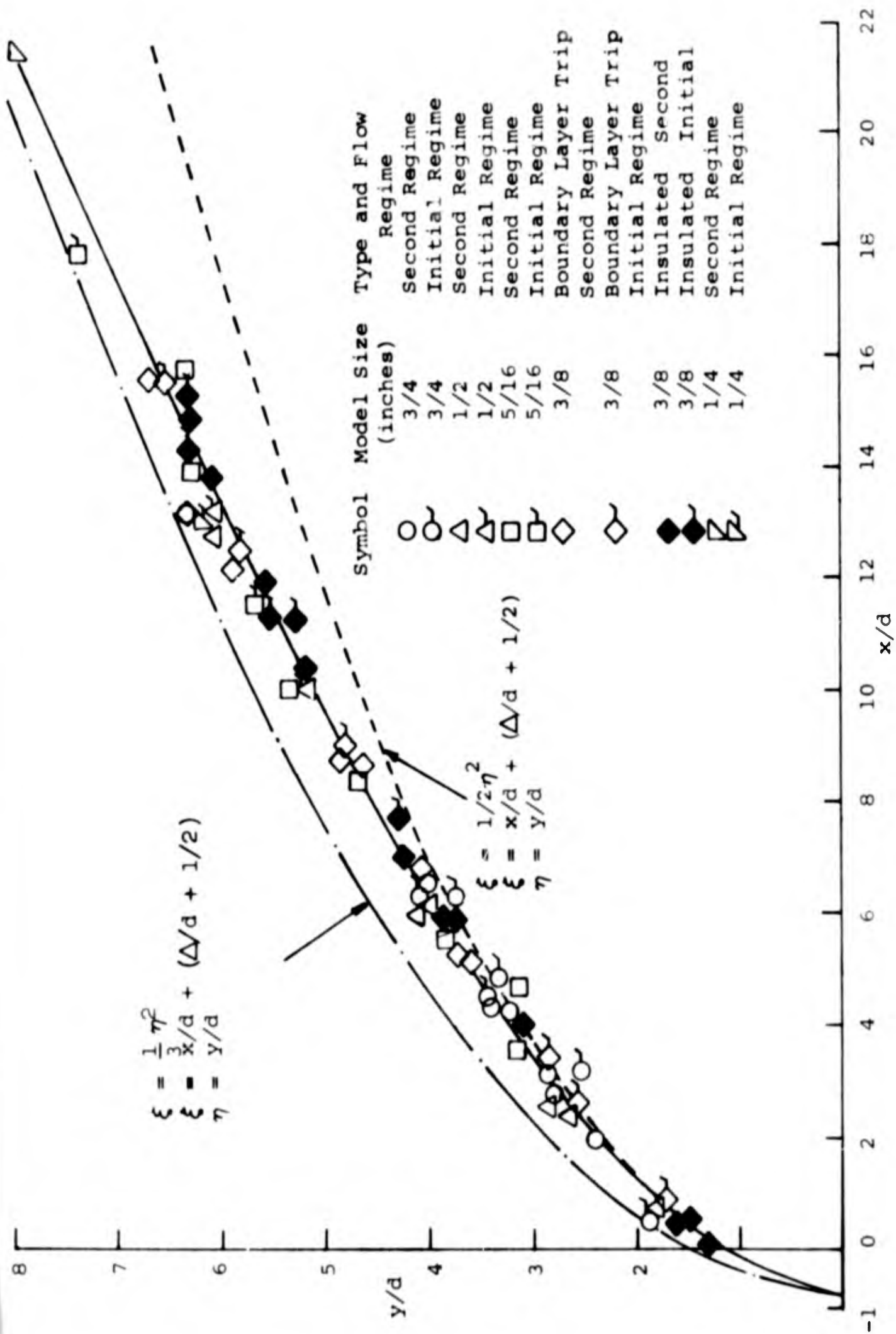


FIGURE 10 - BOW SHOCK WAVE SHAPE

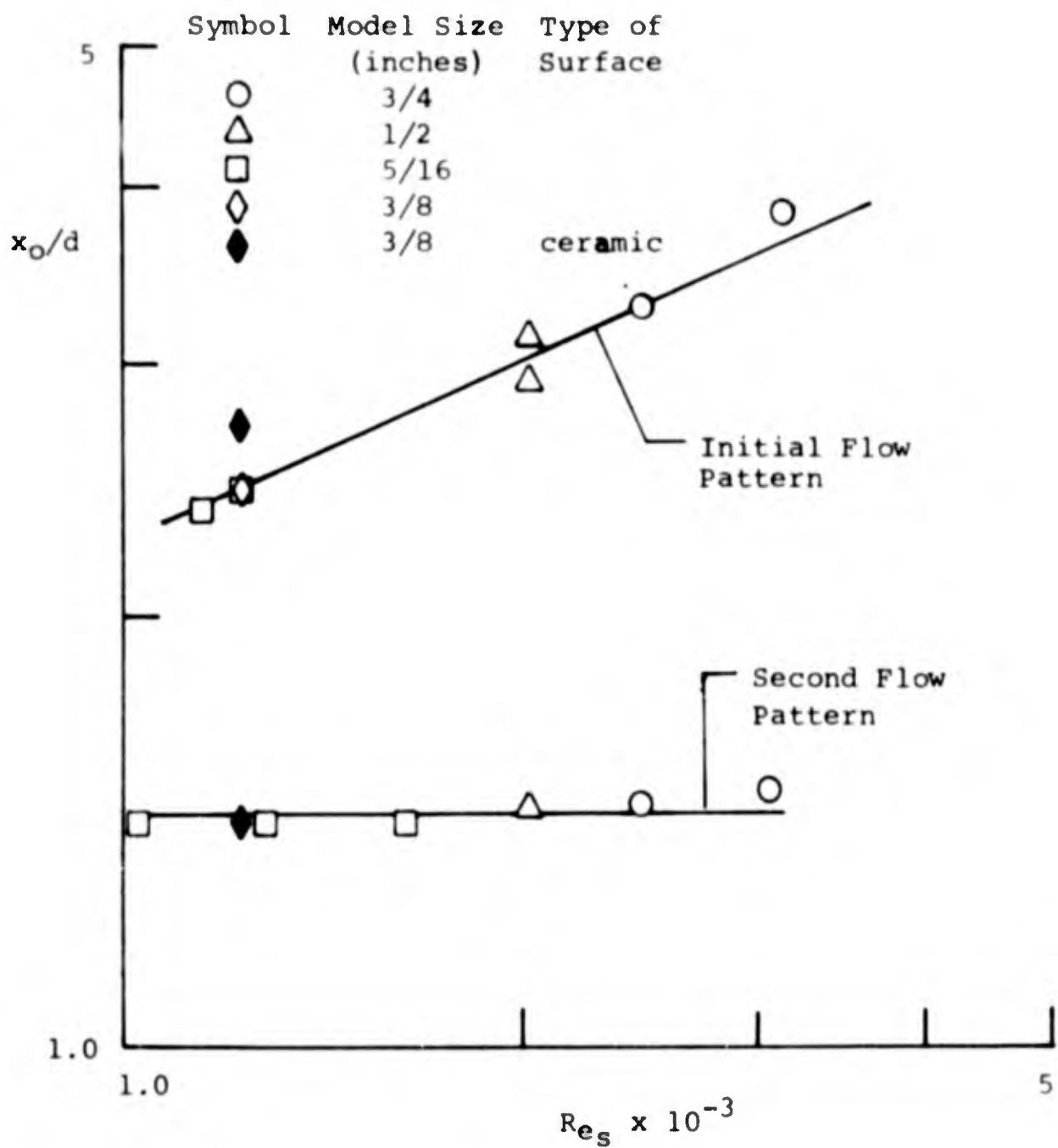


FIGURE - 12 DISTANCE TO WAKE NECK vs. REYNOLDS NUMBER:
INITIAL AND SECOND FLOW PATTERNS

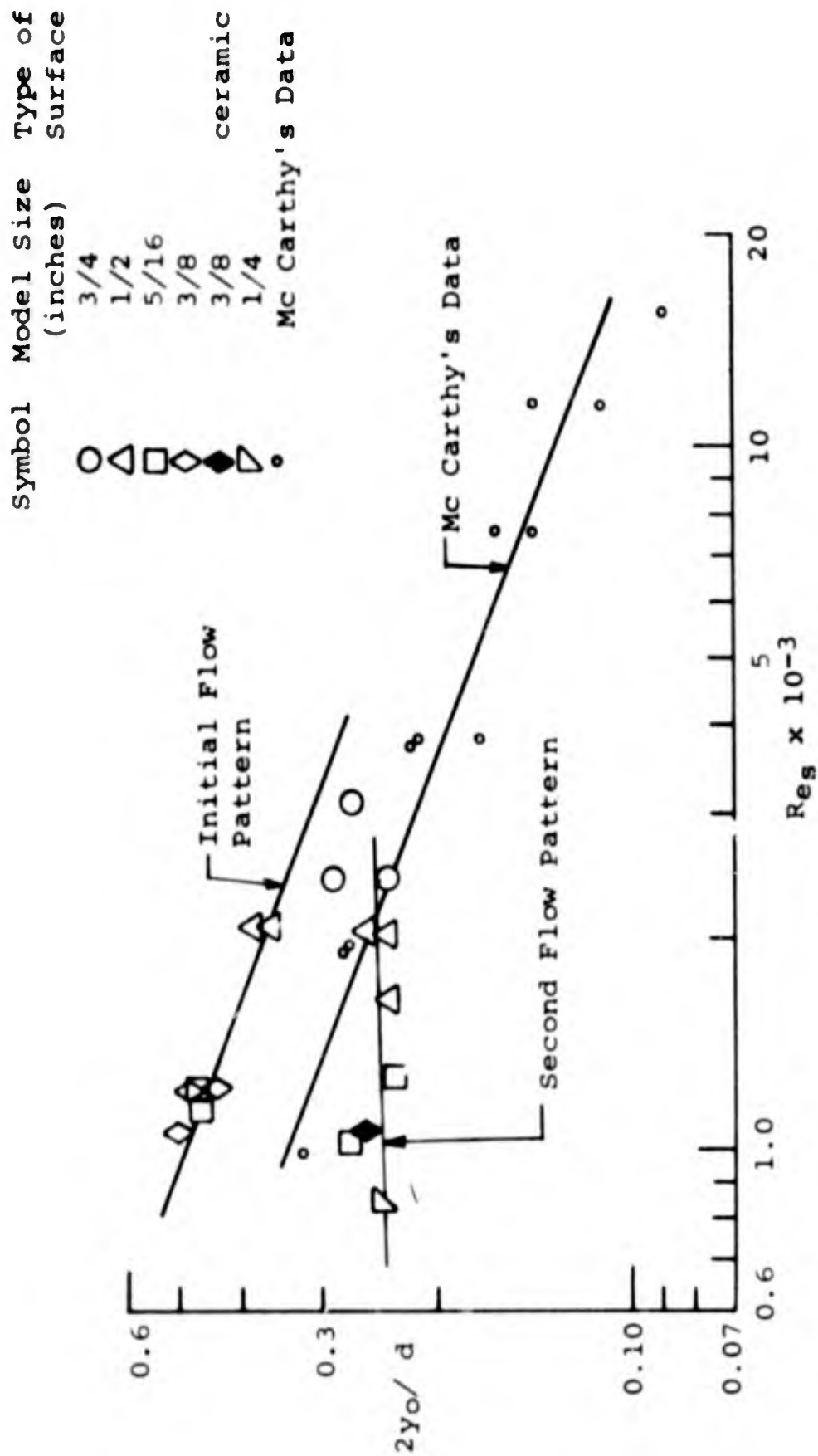
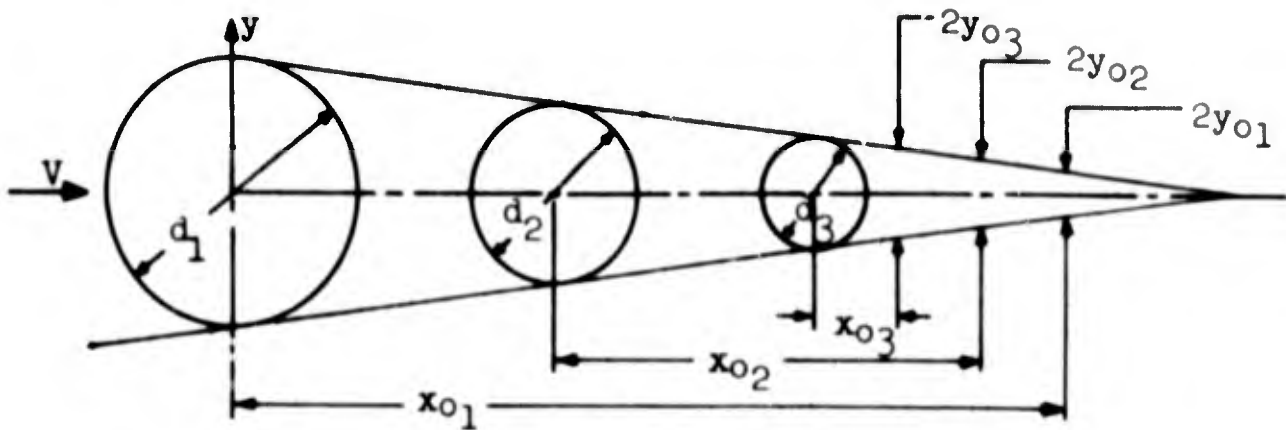
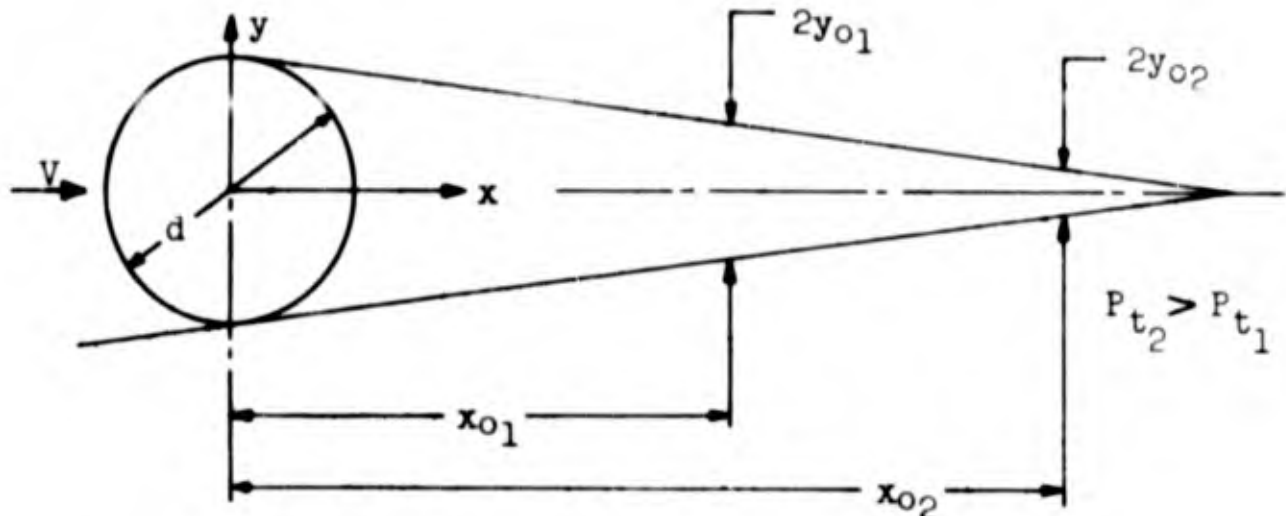


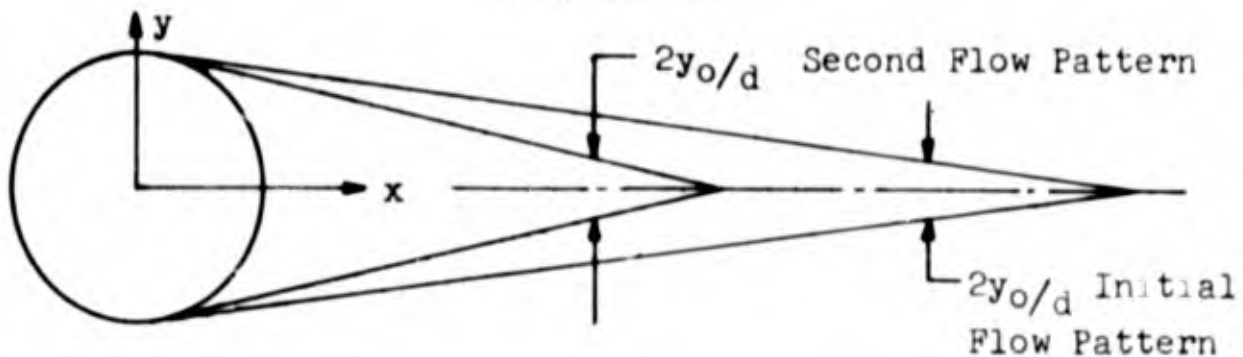
FIGURE - 13 WAKE NECK WIDTH vs. REYNOLDS NUMBER: INITIAL AND SECOND FLOW REGIMES



a--MODEL DIAMETER EFFECT AT CONSTANT P_t ; INITIAL FLOW REGIME



b--REYNOLDS NUMBER EFFECT AT CONSTANT DIAMETER; INITIAL FLOW REGIME



c--COMPARISON OF INITIAL AND SECOND FLOW REGIMES FOR IDENTICAL REYNOLDS NUMBERS

FIGURE 14- EFFECT OF REYNOLDS NUMBER AND MODEL DIAMETER ON SHEAR LAYER GEOMETRY

During the second flow regime the nondimensionalized distance to the wake neck and the nondimensionalized wake width are constant, as shown on Figures 12 and 13. Defining an angle θ which is then computed assuming straight shear layers, one finds this angle to be constant for both flow regimes, the second regime exhibiting a larger θ than the initial regime. (Figure 15). Thus for a given Reynolds Number and model diameter the two cases are shown in Figure 14 (c) for comparison.

Demetriades, (Ref.10) through the use of the hot wake anemometer, found Reynolds Number independence for the nondimensionalized wake width of the turbulent wake. His result agrees well with the results in the second flow regime.

Shown on Figure 13 is the result obtained by McCarthy (Ref. 15). His data was obtained at Mach Number 5.85 and in a known laminar flow. Agreement between McCarthy's data and that obtained during the initial flow pattern should be noted.

WAKE SHOCK WAVE

The shape of the secondary or wake shock wave is a function of local Mach Number and the turning angle for the inviscid flow produced by the shear layer and viscous wake. Figure 16 illustrates the shape of this shock wave in the region where it is relatively straight, that is between its formation by the coalescence of weaker waves and where it experiences a higher Mach Number flow further from the body. From previous discussion, no changes in the neck region could be determined during the second flow regime. The wake shock shape determined for the second flow regime is therefore constant regardless of model size, surface condition, or Reynold's Number.

Figure 17 illustrates the wake shock wave shape for the initial flow pattern, with the wake shock wave shape for the second shock wave shape superimposed for comparison purposes.

Symbol	Model Size (inches)	Type of Surface
○	3/4	
△	1/2	
□	5/16	
◇	3/8	
◇	3/8	Boundary layer trip

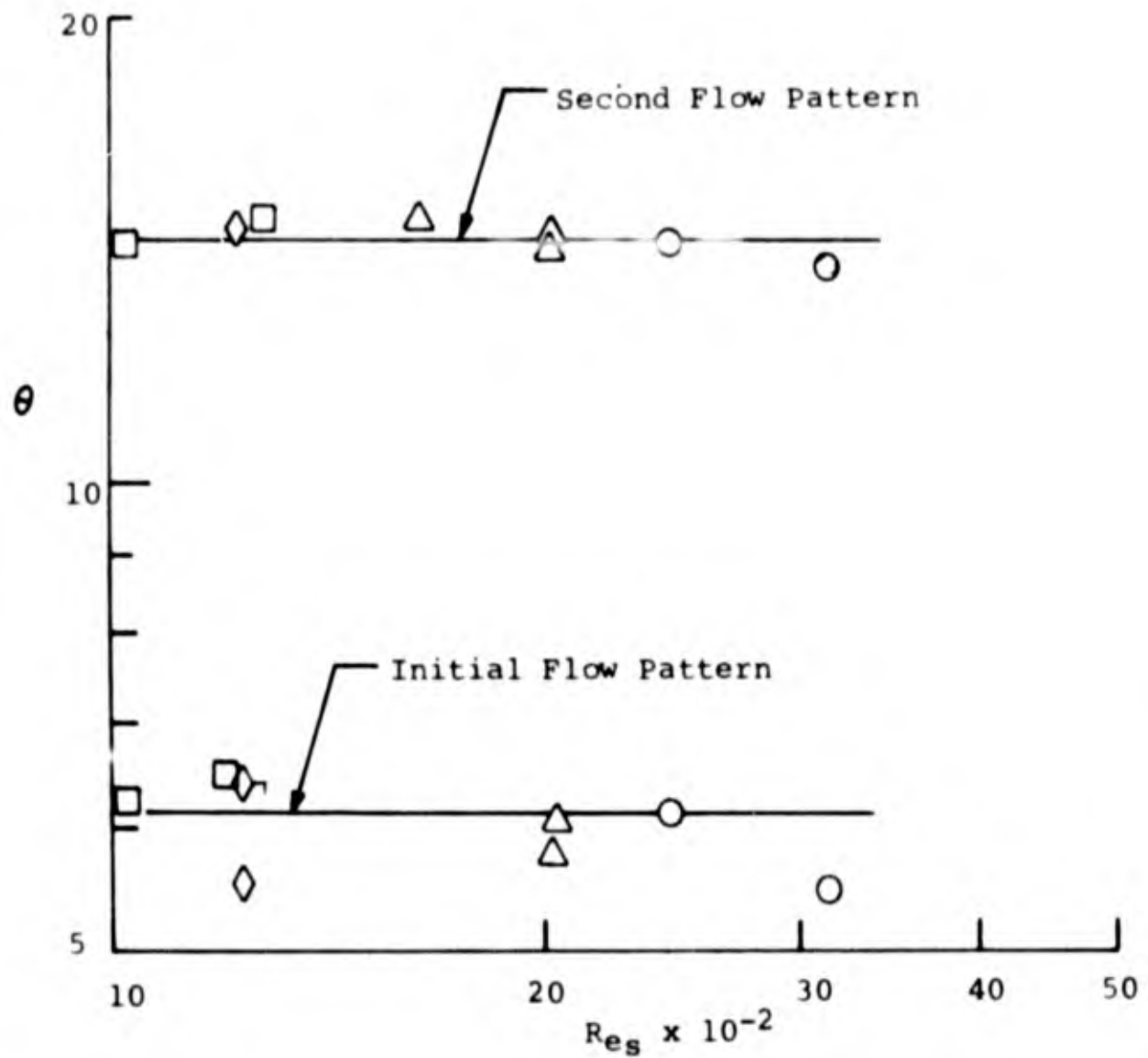


FIGURE - 15 SHEAR LAYER ANGLE vs. REYNOLDS NUMBER:
INITIAL AND SECOND FLOW PATTERNS

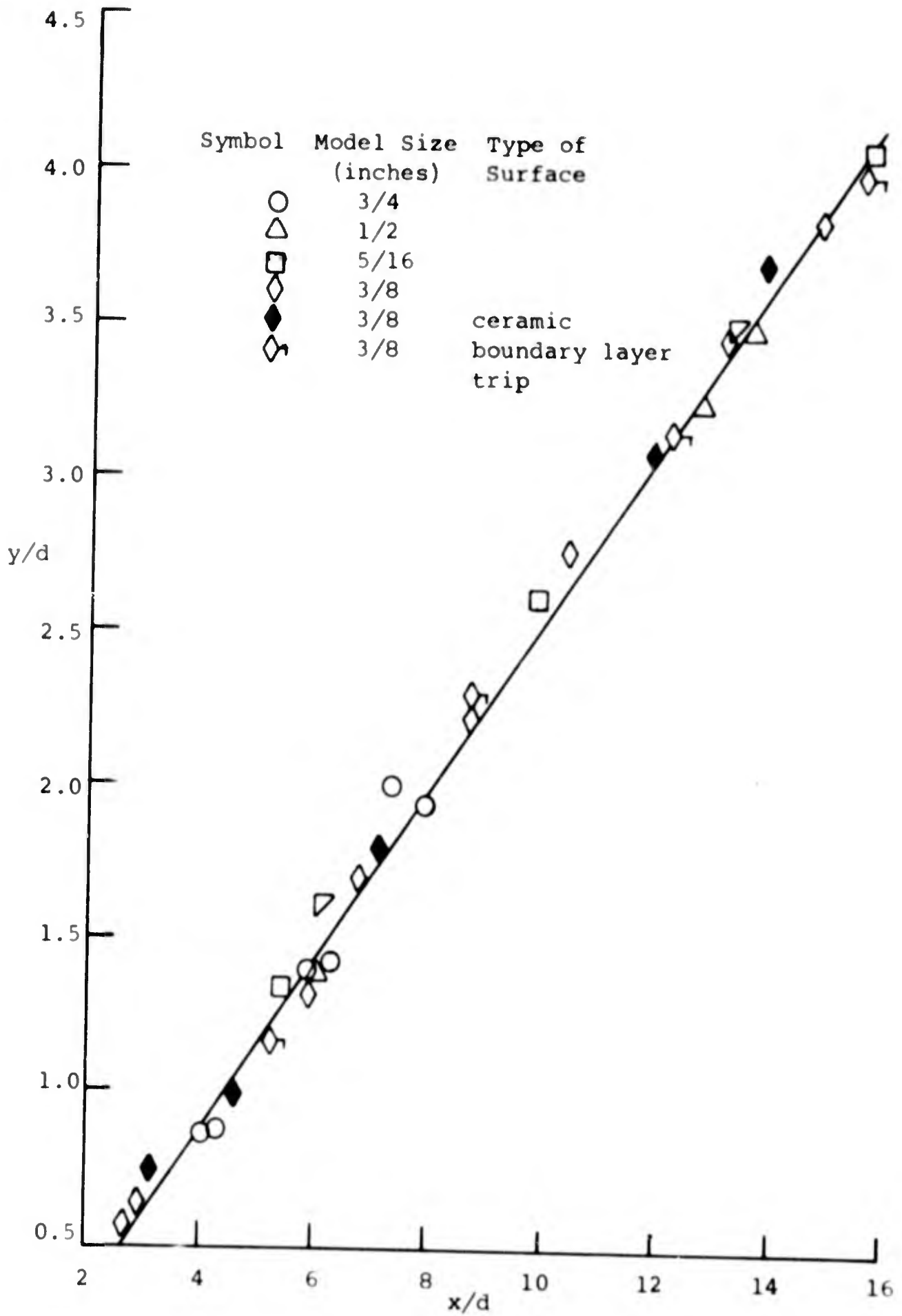


FIGURE 16 - WAKE SHOCK SHAPE: SECOND FLOW PATTERN

The variation in the wake shock wave is in agreement with results which were discussed previously for the initial flow pattern. The wake shock wave, with increased Reynolds Number, proceeds to larger values of x/d as does the wake neck, and also experiences decrease in y/d as does the wake neck. The inclination angle of the straight portion of the wake shock waves is constant regardless of Reynolds Number in the initial flow regime. Again, these straight shock wave portions were obtained between the coalescence of weaker waves region outward to the regions wherein the Mach Number increases and the shock strength falls off.

INITIAL WAKE GROWTH

No wake growth data was obtainable in the second flow regime since the wake edge as defined by Schlieren technique is non-descript for this flow pattern. (See Figure 5).

Wake growth for the initial flow pattern is given on Figure 18. For this case the initial data points follow the Reynolds number dependence shown to dominate in the wake neck region. In this region, as in the shear layers, the flow appears to follow a self similarity. The growth has been linearized since the slight initial curvature is difficult to ascertain through schlieren techniques. Commensurate with the low speed power law analogy, $x/d = (y/d)^m$, the data points are shown to fall off to a lower growth rate as x/d increases. The curves were not extended through these points. Since it is felt they are incorrect, although they indicate the proper trend, the error occurs partially due to inadequate Schlieren sensitivity.

THE INITIAL FLOW PATTERN

By way of recapitulation, the initial flow pattern is characterized by a bow shock wave which is independent of Reynolds Number in regard to both its shape and stand-off distance. Proceeding downstream, there is found a shock system issuing

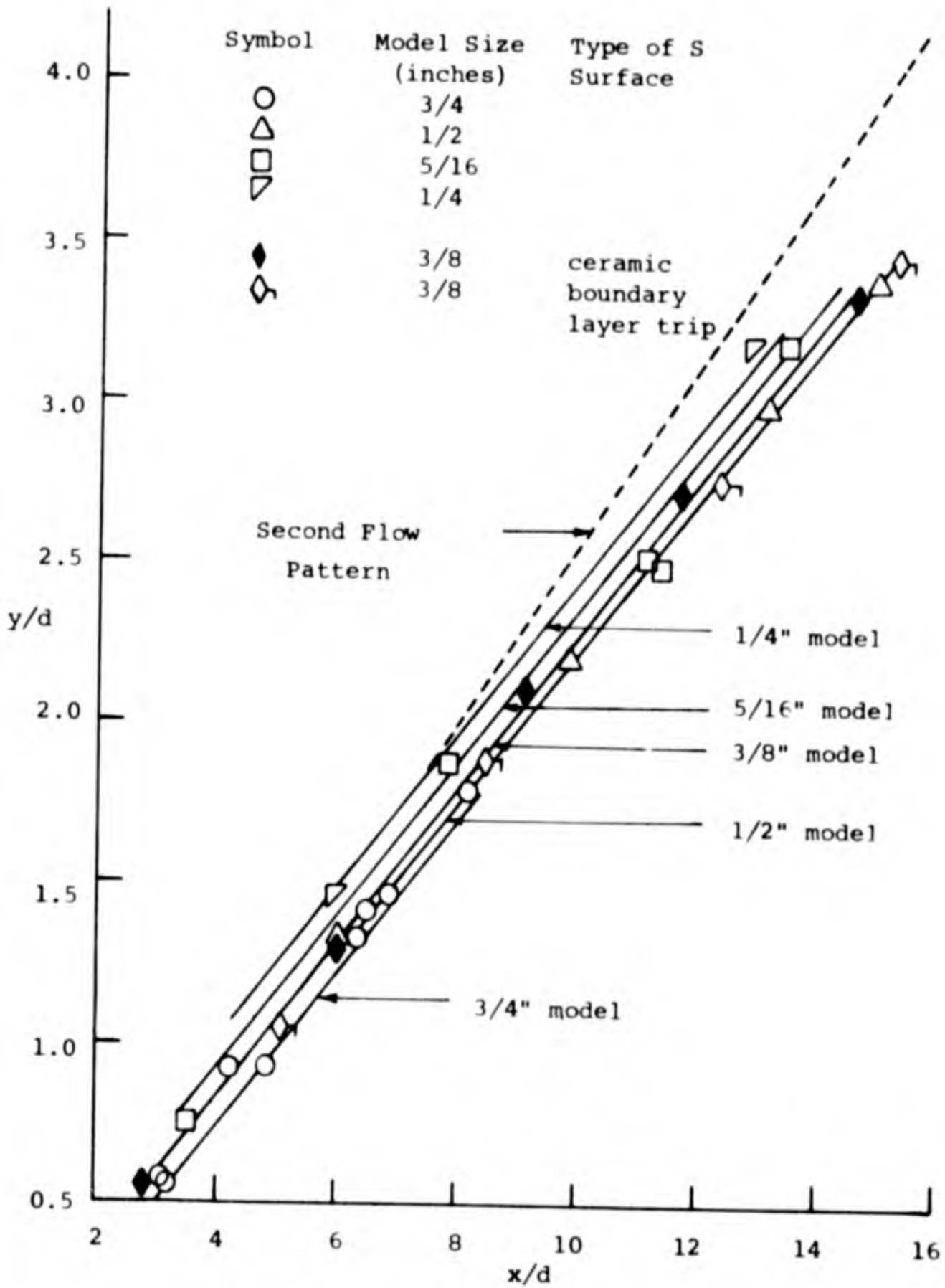


FIGURE 17 - WAKE SHOCK SHAPE: INITIAL FLOW PATTERN

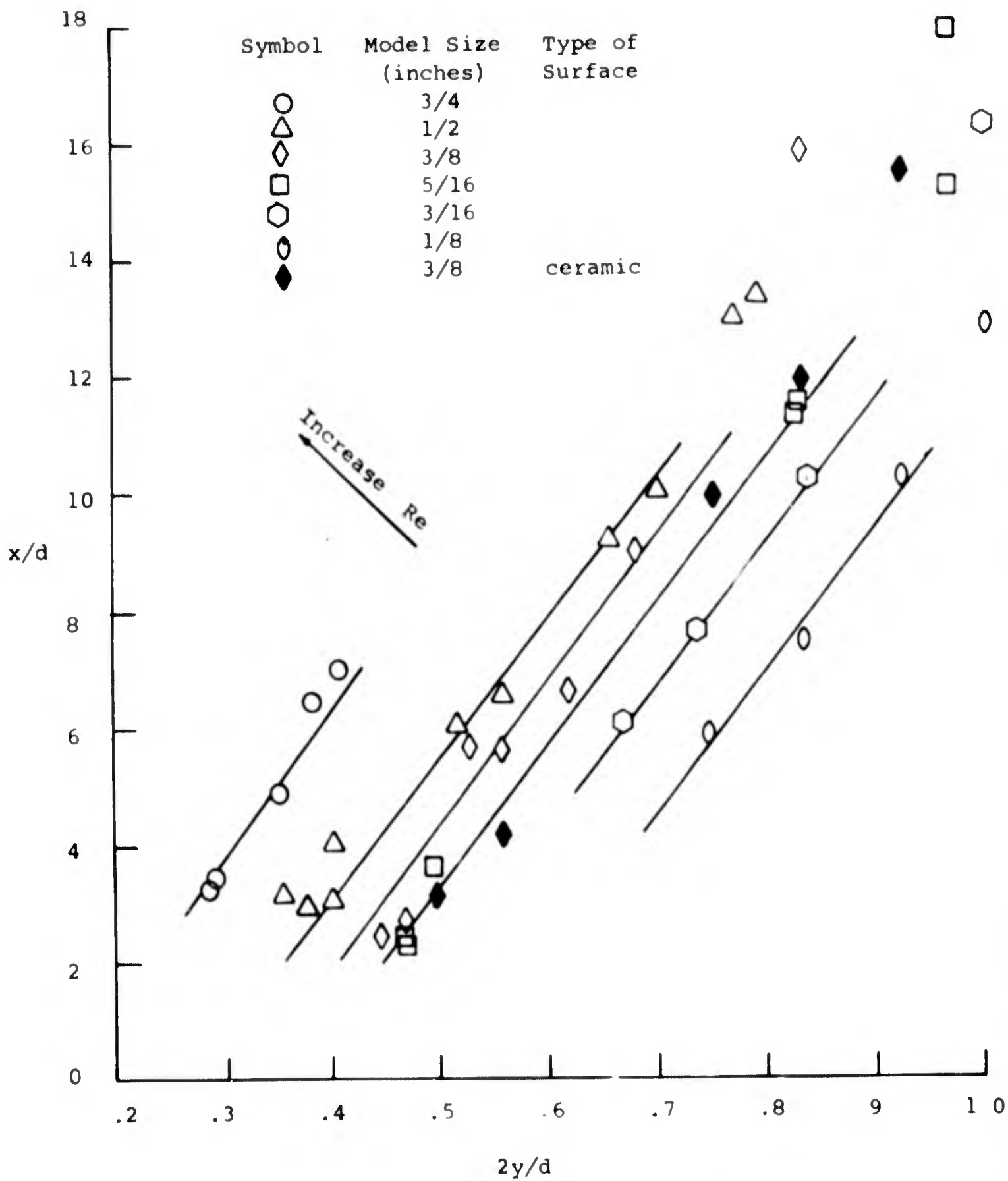


FIGURE 18 - WAKE GROWTH'S INITIAL FLOW PATTERN

from the body surface. Between the boundary layer separation region and the reattachment region the shear layers, (which are relatively straight), follow a sort of scaling law as defined by the sketches drawn on that section of the discussion. This scaling law being in part dependent on $(R_e)^{-1/2}$ as seen from the slopes of Figures 12 and 13. Downstream of the wake neck the wake width retains this scale effect as it assumes a particular growth rate. Further downstream in the wake there appears to occur laminar to turbulent transition. Comparison with published data results in the strong possibility that this initial flow regime contains laminar flow far downstream in the wake until transition occurs there.

THE SECOND FLOW PATTERN

It must be emphasized that under no conditions was it possible to obtain tunnel operations without the appearance of this flow regime. Further, this regime constituted 90 to 95 percent of each tunnel run.

Similar to the initial flow pattern, the second flow pattern was characterized by a bow shock wave which did not depend on Reynolds number with respect to its shape or stagnation point shock layer thickness. The boundary layers separating from the body combined to form the wake. The entire shear layer region appears to be free of Reynolds Number effects in regard to flow geometry. An analysis of the base flow region similar to that offered by Chapman, Kuehn, and Larson(Ref. 16), would suggest the possibility of turbulent flow in this regime. However, even under this hypothesis the question remains as to where the laminar to turbulent transition occurs. Three distinct possibilities exist. The transition mechanism could occur in either the boundary layers before separation, in the shear layers between boundary layer separation and reattachment at the wake neck, or at the wake neck and downstream. The findings thus far reduce the possibilities to the first and second offered, due to the shear layer geometry.

IV CONCLUSIONS

BOW SHOCK WAVE STAND OFF DISTANCE

Theory differs widely as to the effect of Reynolds number on the bow shock wave stand off distance. The Reynolds number range covered by this report is not broad enough to establish definite independence of this parameter, however, it can be stated that the effect of Reynolds number is either very small or non-existent, in the Reynolds number range obtained.

INITIAL AND SECOND FLOW REGIMES

By comparison to existing results in both the laminar and turbulent wake and since thermal effects on the body aided in the transition from the initial to the second flow regime, there is a strong possibility that these two regimes represent laminar and turbulent flows respectively. In order that this point be clarified, additional experimental work is necessary. If this hypothesis is true, only a turbulent wake is obtainable behind a two-dimensional cylinder in the facility employed for these tests, since the initial flow pattern exists for only short time periods. Throughout the literature dealing with hypersonic wakes more explicit information regarding the location of the laminar to turbulent transition is required. Reference 17, in dealing with the width of the wake neck, appears to agree with the results obtained in the second flow regime, and thus may well be discussing the case wherein transition occurs before the wake neck.

SUGGESTIONS FOR FUTURE INVESTIGATION

As indicated in the introduction to this report, the Schlieren observations herein reported are preliminary to the design of explicit investigations. As a result of the data

herein reported, the following measurements are suggested.

1. Hot wire anemometer investigation of both the free stream (tunnel turbulence level), and the flows in the second flow regime including the boundary layer, shear layers, base flow region, and near wake.
2. Pressure measurements at body surface, in the base flow region, and in near wake.

It should be noted that just such measurements are being undertaken and will be embodied in a second ARL report on this topic.

V BIBLIOGRAPHY

Dana, T.A., and Short, W.W., "Experimental Study of Hypersonic Turbulent Wakes", Report to Army Rocket and Guided Missile Agency on Contract No. DA-04-495-ORD-3112, 1961.

Fay, J.A., and Goldburg, A., "The Unsteady Hypersonic Wake Behind Spheres", American Rocket Society 17th Annual Meeting and Space Flight Exposition, Preprint 2676-62, 1962.

Hayes, W.D., Probstein, R.F., Hypersonic Flow Theory, Academic Press, New York and London, 1959.

Howarth, L., Modern Developments in Fluid Dynamics, High Speed Flow, Oxford University Press, London, 1956.

Hung-Ta, H. and Probstein, R.F., "Compressible Viscous Layer in Rarefied Hypersonic Flow", Proceedings of the 2nd International Symposium on Rarefied Gas Dynamics, 1960.

Jack, F.R., and Diaconis, N.S., "Effect of Heating and Cooling on Transition", NACA TN 3562, 1955.

Kendall, J.M., "Experimental Study of Cylinder and Sphere Wakes at a Mach Number of 5.7", Jet Propulsion Laboratory Report No. 32-363, 1962.

Lees, L., "Hypersonic Wakes and Trails", American Rocket Society 17th Annual Meeting and Space Flight Exposition, Nov. 13-18th, 1962.

Lees, L., and Hromas, L., "Turbulent Diffusion in the Wake of a Blunt Nosed Body at Hypersonic Speeds", Journal of the Aerospace Sciences, Vol. 29, No. 8, 1962, pp. 976-993.

Lees, L. and Probstein, R.E., "Hypersonic Flow of a Viscous Fluid", Report to the Aeronautical Research Laboratory, WPAFB, on Contract AF 33(038)-250, 1953.

Probstein, R. and Kemp, N., "Viscous Aerodynamic Characteristics in Hypersonic Rarefied Gas Flow", Journal of the Aerospace Sciences, Vol. 27, No. 3, March 1960, p. 174.

Schlichting, H., Boundary Layer Theory, Fourth Edition, McGraw-Hill Book Co., Inc. New York, 1960.

Vandriest, E.R., and Boison, C.J., "Experiments on Boundary Layer Transition at Supersonic Speeds", Journal of Aeronautical Sciences, Vol. 24, pp. 885-899, 1957.

Vibicans, G., "Motion of a Pair of Vortices Behind a Cylinder", U.S. Naval Weapons Laboratory Report No. 1794, 1962.

VI REFERENCES

1. Tepe, F.R., Brown, D.L., Token, K.H., and Hoelmer, W., "Theoretical Operating Ranges and Calibration Results of the ARL Twenty-Inch Hypersonic Wind Tunnel", ARL 63-189, October 1963.
2. Brown, D.L., Token, K.H., Hoelmer, W., and Tepe, F.R., "Instrumentation and Recording Equipment Used in Conjunction with the ARL Twenty-Inch Hypersonic Wind Tunnel", ARL 63-162, September 1963.
3. Gregorek, G.M., and Lee, J.D., "Design Performance and Operation Characteristics of the ARL Twenty-Inch Hypersonic Wind Tunnel", ARL 62-392, August 1962.
4. Gregorek, G.M., and Lee, J.D., "Initial Calibrations and Performance of the ARL Twenty-Inch Hypersonic Wind Tunnel", ARL 62-393, August 1962.

5. Goll, M.E., and Lapenos, T.A., "Operation and Maintenance Instructions, Off Axis Double Pass Schlieren System", ARL 62-463, 1962.
6. Ladenburg, R.W., Lewis, B., and Pease, R.M., Physical Measurements in Gas Dynamics and Combustion, Vol. IX, High Speed Aerodynamics and Jet Propulsion, Princeton University Press, N.Y. 1952.
7. Holden, D.W., Pankhurst, R.D., Wind Tunnel Technique, Sir Isaac Ditman and Sons, Ltd., London, 1952.
8. Kodak Reference Handbook, Eastman Kodak Co., Rochester, New York, Copyright, 1946.
9. Slattery, R.E., and Clay, E.G., "The Turbulent Wake of Hypersonic Bodies", American Rocket Society, 17th Annual Meeting and Space Flight Exposition, Pan American Auditorium, Los Angeles, California, Nov. 13-18, Preprint No. 2673-62, 1962.
10. Demetriades, A., "Some Hot-Wire Anemometer Measurements in a Hypersonic Wake", Proceedings of the Heat Transfer and Fluid Mechanics Institute, University Press, 1961.
11. Chester, W., "Supersonic Flow Past a Bluff Body with a Detached Shock", Journal of Fluid Mechanics, Vol. 1, Part 4, October 1956, p. 353.
12. Probstein, R.F., "Inviscid Flow in the Stagnation Point Shock Region of Very Blunt Bodies at Hypersonic Flight Speeds", Report to the Aeronautical Research Laboratory, WPAFB, on Contract AF 33(616)2798, 1956
13. Ambrosis, A. and Wortman, A., "Stagnation point Shock Detachment Distance for the Flow Around Spheres and Cylinders in Air",

Journal of the Aerospace Sciences, Vol. 29, 1962, p. 875.

14. Oguro, H., and Hannah, B.W., "Photomultiplier Applications to Hypersonic Flow Research", to be released as an ARL Report, 1964.
15. McCarthy, J.F., "Hypersonic Wakes", Graduate Aeronautical Laboratories, California Institute of Technology, Hypersonic Research Project, Memorandum No. 67, 1962.
16. Chapman, D.R., Kuehn, D.M., and Larson, H.K., "Investigation of Separated Flows in Supersonic and Subsonic Streams with Emphasis on the Effect of Transition", Ames Aeronautical Laboratory, NASA Report 1356, 1958.
17. Morretti, G., and Byrne, R., Hypersonic Flow Field Calculations - Three Dimensional and Real Gas Flows", The High Temperature Aspects of Hypersonic Flow, Pergamon Press, The MacMillan Company, New York, 1964.